

Related topics

Spontaneous and stimulated light emission, inversion, collision of second type, gas discharge tube, resonator cavity, transverse and longitudinal resonator modes, birefracton, Brewster angle, Littrow prism, Fabry Perot Etalon.

Principle and task

The difference between spontaneous and stimulated emission of light is demonstrated. The beam propagation within the resonator cavity of a He-Ne laser and its divergence are determined, its stability criterion is checked and the relative output power of the laser is measured as a function of the tube's position inside the resonator and of the tube current.

By means of a birefringent tuner and a Littrow prism different wavelengths can be selected and quantitatively determined if a monochromator is available.

Finally you can demonstrate the existence of longitudinal modes and the gain profile of the He-Ne laser provided an analysing Fabry Perot system is at your disposal.

Equipment

Exp.Set-Helium-Neon Laser, basic set	08656.01	1
Exp.Set-He-Ne Laser, advanced options	08656.02	1
Vernier caliper	03010.00	1
Measuring tape, l = 2 m	09936.00	1

Problems

1. Set up the He-Ne laser. Adjust the resonator mirrors by use of the pilot laser. (left mirror: VIS, HR, plane ; right mirror: VIS, HR, R = 700 mm)
2. Check on the stability condition of a hemispherical resonator.
3. Measure the integral relative output power as a function of the laser tube's position within the hemispherical resonator.

4. Measure the beam diameter within the hemispherical resonator right and left of the laser tube.
5. Determine the divergence of the laser beam.
6. Measure the integral relative output power as a function of the tube current.

The He-Ne laser can be tuned using a BFT or a LTP. Longitudinal modes can be observed by use of a Fabry Perot Etalon of low finesse. Remark: These points can only be covered quantitatively if a monochromator and an analysing Fabry Perot system are available.

Set-up and procedure

The experimental set-up is shown in Fig. 1. The adjustment of the resonator mirrors has to be performed as described in the manual as well as the alignment of the birefringent tuner (BFT), the Littrow prism (LTP) and the Fabry Perot Etalon (FPE). Once the basic adjustment has been done, the first experiments can be executed.

The optical resonator of the He-Ne laser is designed according to the given active material (Ne) and the required beam quality.

The objective is to achieve the best possible beam output in the basic Gaussian mode (TEM_{00}).

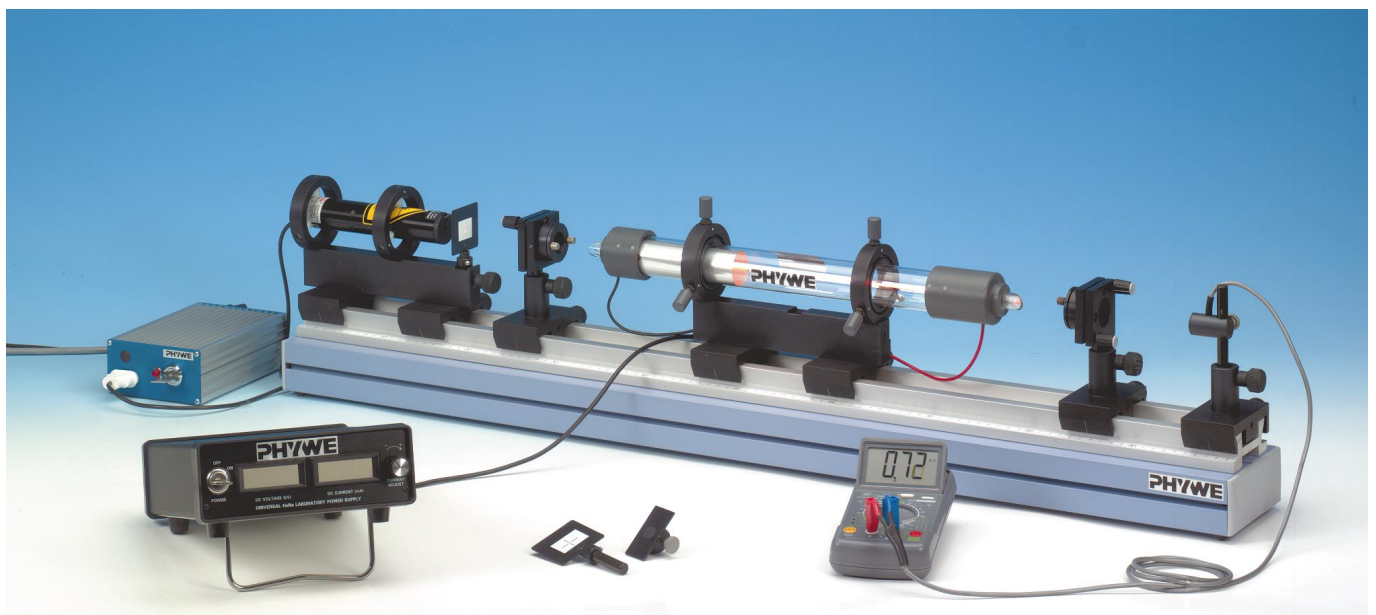
Generally speaking these are two contradictory requirements since a high power output requires the use of a large volume of active material, whereas the fundamental mode is restricted to its own volume.

This is why the hemispherical resonator has the optimal configuration for the He-Ne laser.

This can be explained by characteristics of Gaussian beams. The beam radius w (w =waist) is a result of the following relationship:

Caution: Never look directly into a non attenuated laser beam

Fig. 1: Experimental set-up of He-Ne laser system.



$$w(z) = w_0 \cdot \sqrt{1 + \left(\frac{z}{z_R}\right)^2}$$

w_0 is the smallest beam radius at the minimum of the beam waist and z_R is the Rayleigh length.

$$z_R = \pi \cdot \frac{w_0^2}{\lambda}$$

Fig. 2 shows the relationship between the beam diameter and the length z . z points in the direction in which the beam is propagating.

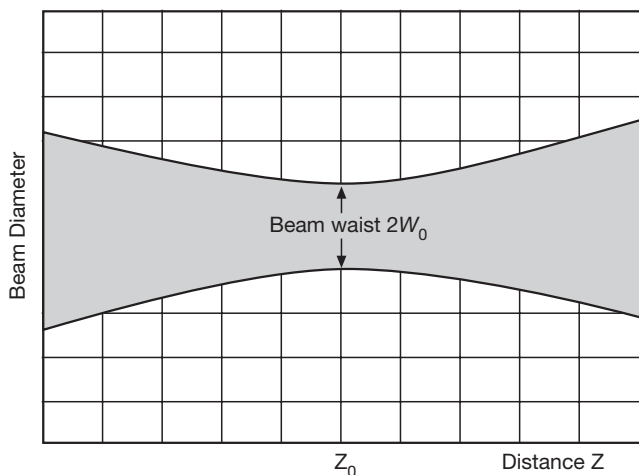


Fig. 2: The beam diameter of a Gaussian beam in the fundamental mode.

The beam's radius is smallest at the location z_0 . The beam radius increases linearly as the distance increases. Since light waves are spherical waves a radius of curvature of the wave front can be allocated to each location z . The radius of curvature $R(z)$ can be calculated with the following relationship:

$$R(z) = z + \frac{z_R^2}{z}$$

This is illustrated in Fig. 3.

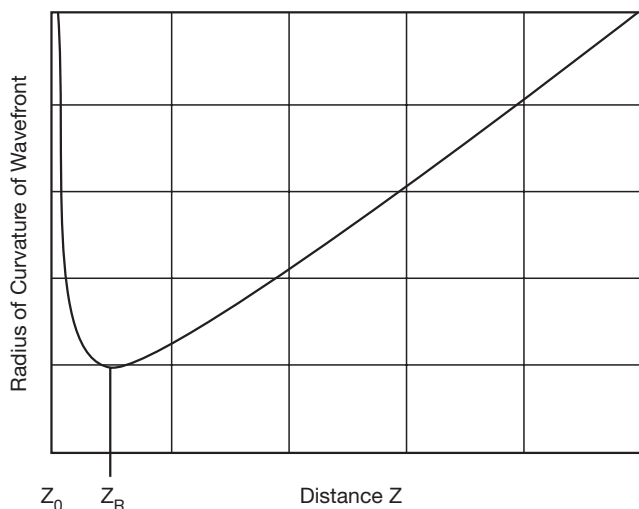


Fig. 3: Radius of curvature of the wavefront versus the distance z from the beam waist at $z = 0$.

At $z = z_R$ the radius of curvature is at a minimum. The radius of curvature at $z = 0$ is infinite. At this point the wave front is plane.

Above the Rayleigh length z_R the radius again increases in linear fashion. This is a basic but important statement. It shows that there is a real parallel beam at only one point of the light wave, that is at its focal point. In the range

$$-z_R \leq z \leq z_R$$

a beam can be considered as parallel or collimated. Fig. 4 shows the Rayleigh range as well as the divergence Θ in the far field.

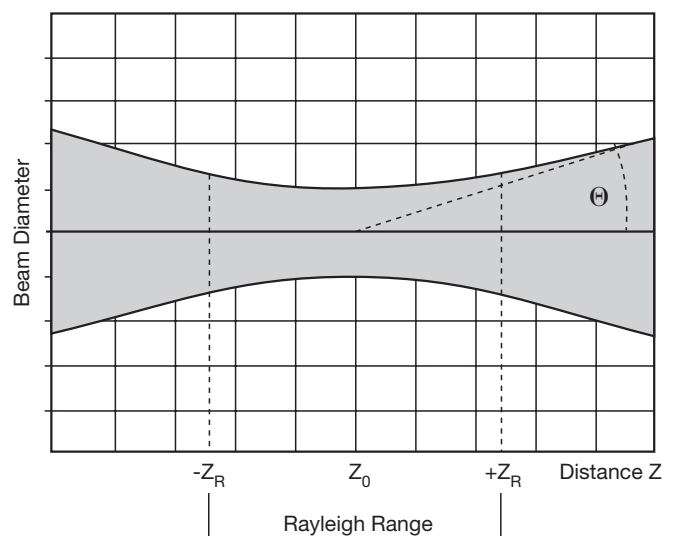
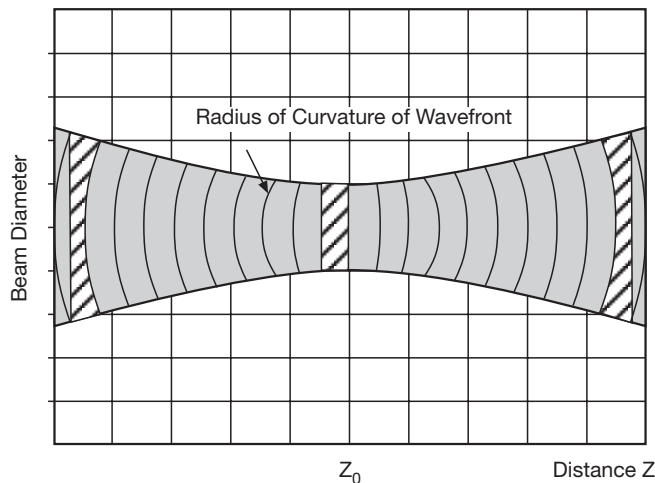


Fig. 4: Rayleigh range and divergence.

When reversing the operation, a stable optical resonator can now be constructed by adapting the radii of curvature in such a way that they correspond to the radii of curvature of the basic Gaussian mode. Fig. 5 shows a spherical and a hemispherical resonator. If a laser is made to oscillate with this kind of configuration the beam path can be calculated with the above mentioned equations based on the knowledge of the mirror radii and the distance between the mirrors. Due to the demand for a high output power in the fundamental mode, a spherical arrangement is out of question for the He-Ne laser. Transverse modes can also oscillate in spherical resonators. The fundamental mode could be achieved in this type of resonator by putting a diaphragm inside the resonator which only allows the fundamental mode to pass freely. However, this option is complicated. The hemispherical resonator is chosen because the place of the plane wave front is very well defined. Only the fundamental mode is reflected back with low losses.

Fig. 5: Construction of an optical resonator with mirrors. The resonator has the same radii of curvature as the fundamental Gaussian mode at particular points of z .



Moreover, the He-Ne laser requires a narrow capillary. The recombination process of the laser cycle takes place on its walls. As far as the active material is concerned, the diameter of the capillary should be as small as possible to enable an optimal laser output, but it should not be too small as to block the path of the fundamental mode. The course which the beam radius of the mode takes is determined by the radii of curvature of the distance between the mirrors. However, the mode volume, i.e. the volume filling up the fundamental mode, or the length of the amplifying material should be as large as possible to get as much output as possible from the active material. Long tubes are therefore used in He-Ne lasers to increase the output power. At the same time, the radius of the spherical mirror should be large enough for this purpose. The basic adjustment of the laser with a birefringent tuner (BFT) is explained in the manual. The BFT must be set up in the resonator at a place where the laser beam is parallel "as far as possible". The points made on the selective effect of a BFT are based on observations made on collimated beams. Additional losses could be formed for the weak lines (lines of small gain) which can be minimised by the optimal position of the BFT within the resonator. If no oscillation of the weak lines can be achieved, the following points must be checked and changed accordingly. All optical surfaces, including the surface of the BFT, must be well cleaned. The BFT must be adjusted to the Brewster angle to the optical axis. The discharge current should not be more than 5 mA. The BFT element consists of a natural quartz plate approx. 1 mm thick. When the BFT is placed into the resonator it causes a beam displacement. Therefore it is necessary to repeat the primary alignment when the tuner is used. If the plate is rotated around its optical axis the main line (632.8 nm) will occur three to four times. Select the best one and realign the laser for best operation. When you tune in the vicinity of the main line at 632 nm you will find five different lines at the following wavelengths and relative gains:

1.	611.8 nm	10
2.	629.8 nm	20
3.	632.8 nm	100
4.	635.2 nm	6
5.	640.1 nm	34

The orange line at 611.8 nm as well as the line at 635.2 nm are sensitive to additional losses due to pollution on the optics. Clean them again if you can not find these lines. Especially the windows of the tube and the BFT plate are exposed to pollution because the electrical field of the laser beam on their surfaces is not zero as on the mirrors. Once the orange line is oscillating realign the laser resonator and optimise the Brewster angle by turning the BFT slightly. Note that the line can vanish and will return by slightly turning the plate.

Theory and evaluation

The He-Ne laser was the first continuous working laser. It was invented by Javan et al. in 1961. The fascination for inert gases and their clear atomic structure formed the basis for many spectroscopic investigations. The knowledge obtained through spectroscopic data was extremely helpful in deciding to choose Helium and Neon for the first lasers, using Schawlow Towne's discovery of lasing conditions in 1958 to estimate whether an inversion was feasible in laser operation. The lifetimes of the s- and p-states were well known. Those of the s-states were longer than those of the p-states by a factor of ten. The inversion condition was therefore fulfilled, for the time-being.

Fig. 6 shows the reduced energy-level diagram for Helium and Neon. Only those levels important in the discussion of the excitation and laser processes at a wavelength of 632 nm are indicated.

The left side of the representation shows the lower levels of the Helium atoms. Observe how the energy scale is interrupted and that there is a larger difference in energy in the recombination process than is evident in the diagram. Paschen's names for the Neon energy levels are used (Paschen's term descriptions are often found as well). The terms are simply numbered consecutively, from bottom to top. A characteristic of Helium is that its first states to be excited, 2^1S_1 and 2^3S_1 are metastable, i.e. optical transitions to the ground state 1^1S_0 are not allowed, because this would violate the selection rules for optical transitions. As a result of gas discharge, these states are populated by electron collisions.

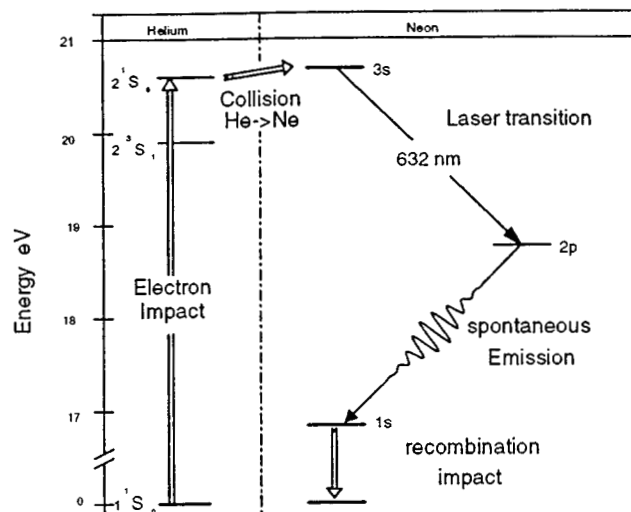


Fig. 6: Excitation and laser process for the visible laser emission.

A collision is called a collision of the second type if one of the colliding bodies transfers energy to the other so that a transition from the previous energy state to the next higher or lower takes place. Apart from the electron collision there is also an atomic collision of the second type. In the latter, an excited Helium atom reaches the initial state because its energy has been used in the excitation of a Neon atom. Both these processes form the basis for the production of a population inversion in the Neon system.

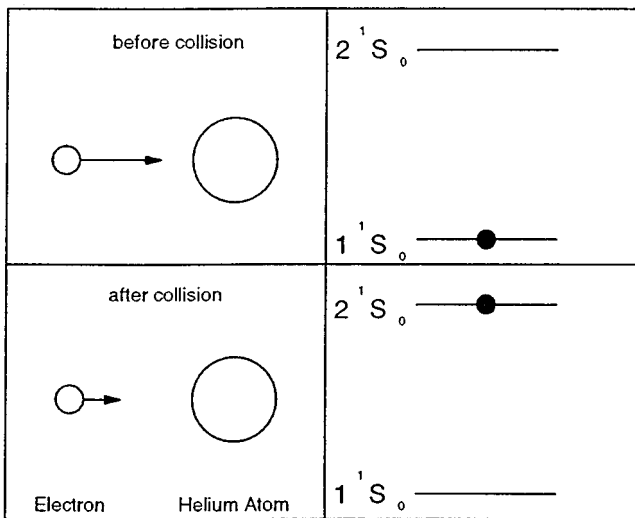
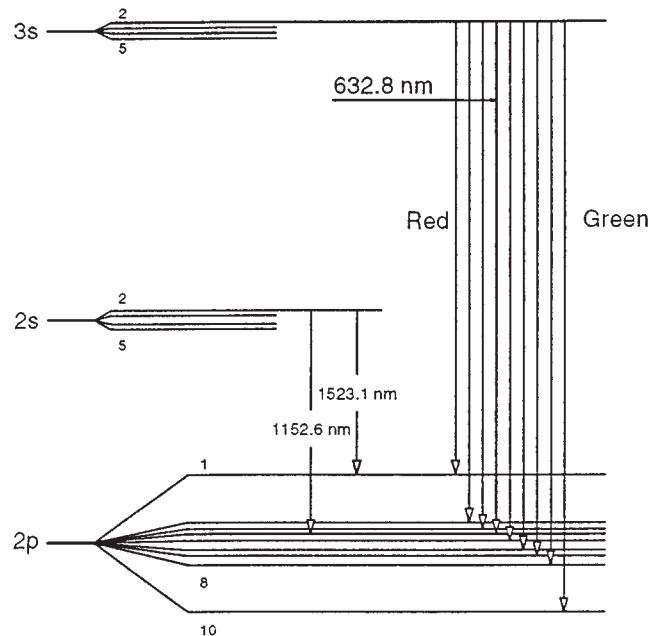


Fig. 7: Electron collision of the second type.

If we look at Fig. 6 we can see that the 2^1S_0 level is slightly below the $3s$ level of the Neon. However, the additional thermal energy kT is sufficient to overcome this gap. As already mentioned, the lifetime of the s -states of the Neon are approximately 10 times longer than those of the p -states. An immediate population inversion between the $3s$ and the $2p$ levels will therefore be generated. The $2p$ level is emptied due to spontaneous emission into the $1s$ level. After this the Neon atoms reach their ground state again, primarily through collisions with the tube wall (capillary), since an optical transition is not allowed. This calming down process is the bottle neck in the laser cycle. It is therefore advisable to choose a capillary diameter that is as small as possible. However, the laser will then suffer more losses. Modern He-Ne lasers work at an optimum under these contradictory conditions. This is the main reason for the comparatively low output of He-Ne lasers. We have discussed the laser cycle of the commonly known red line at 632 nm up to this point. However, the Neon has several other transitions, used to produce about 200 laser lines in the laboratory. The following explanation describes the energy level diagram for further visible lines.

Fig. 8 The most important laser transitions in the Neon system.



The $3s$ state is populated by Helium atoms of the 2^1S_0 state as a result of an atomic collision. The $3s$ state consists of 4 sub-states out of which it is primarily the $3s_2$ state which has been populated through the collision process. The population density of the other $3s$ sub-states is approx. 400 times less than that of the $3s_2$ state. The $2s$ state is populated by the Helium atoms of the 2^3S_1 state as a result of an atomic collision.

The four sub-states of the $2s$ group are all populated in a similar way. Visible (VIS) optical transitions and laser processes take place between the $3s_2 \rightarrow 2p_i$ and infrared (IR) transitions between the $2s_i \rightarrow 2p_i$ energy levels.

The following table shows the most important laser transitions. The Einstein coefficients A_{ik} are given for the visible lines and the gain is indicated as a percentage per meter.

Further laser transitions are known, which start at the $3s_2$ level and terminate at the $3p$ level of the Neon. However, these laser transitions lie even further within the infrared spectral range and cannot be detected with the silicon detector used in the experiment. They are not particularly suitable for experiments. Notice that these lines originate from the same level as the visible lines and are therefore competing with them. Since the cross-section of the stimulated emission is increasing with λ^3 as well, the amplification of these lines is therefore very strong. This applies to the $3.39 \mu\text{m}$ line in particular, which, due to a sufficiently long capillary, shows laser activity (so called superfluorescence) even without an optical resonator.

Transition	Wavelength [nm]	A_{jk} [$10^8 s^{-1}$]	Gain [%/m]
3s2→2p1	730.5 ^③	0.00255	1.2
3s2→2p2	640.1 ^①	0.0139	4.3
3s2→2p3	635.2 ^①	0.00345	1.0
3s2→2p4	632.8 ^①	0.0339	10.0
3s2→2p5	629.4 ^①	0.00639	1.9
3s2→2p6	611.8 ^①	0.00226	1.7
3s2→2p7	604.6	0.00200	0.6
3s2→2p8	593.9	0.00255	0.5
3s2→2p9	★		
3s2→2p10	543.3	0.00283	0.52
2s2→2p1	1523.1 ^②		
2s2→2p2	1177.0 ^③		
2s2→2p3	1160.5		
2s2→2p4	1152.6 ^③		
2s2→2p5	1141.2 ^③		
2s2→2p6	1084.7 ^③		
2s2→2p7	1062.3		
2s2→2p8	1029.8		
2s2→2p9	★		
2s2→2p10	886.5		
2s3→2p2	1198.8 ^③		
2s3→2p5	1161.7 ^③		
2s3→2p7	1080.1 ^③		

Table 1: Transitions and laser lines

- ① Laser transitions are demonstrated in the experiment if the laser tube is supplied with perpendicular windows or Brewster windows
 - ② Laser transition can be demonstrated if the laser tube is supplied with Brewster windows and a special set of mirrors (*)
 - ③ Laser transitions can be demonstrated in the experiment if the laser tube is supplied with Brewster windows and an IR mirror set (*)
- * transitions not allowed
(*) not included in equipment set

Appropriate measures must be taken to suppress the superfluorescence to avoid a negative influence on the visible laser lines.

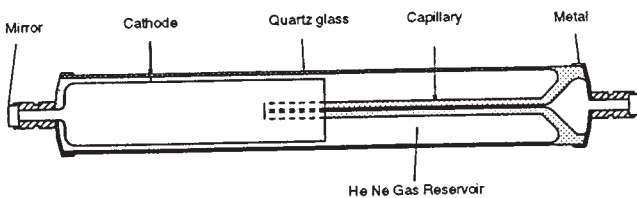


Fig. 9: Modern He-Ne laser with glass-to-metal soldering of the anode, cathode and mirror.

Fig. 9 shows a modern laser tube made with highly perfected manufacturing techniques and optimised to suit the physical aspects of the laser. This applies to the resonator in particular, which is designed for a best possible output in the fundamental mode with a purely Gaussian beam and spectral purity in single longitudinal mode operation (e.g. for interferometric length measurements). The fulfilment of this demand depends, amongst other aspects, on the optimal adaptation of the resonator to the amplification profile of the Neon.

The discharge only burns in the capillary. This is ensured by the expansion and melting of the capillary with the glass tube. The window flange on the anode side is made completely out of glass, to prevent coming into contact with the harmful high voltage during the required cleaning work. The tube being used has an ignition voltage of approx. 8 kV and an operating voltage of approx. 2 kV. The optimal current for the 632 nm line is 5 mA. The Neon atoms move more or less freely in the laser tube but at different speeds. The number N of Neon atoms with the mass m , within a speed interval of v to $v+dv$ is described according to the Maxwell-Boltzmann distribution (Fig. 10).

$$\frac{n(v)}{N} = \frac{4}{\sqrt{\pi}} \cdot \frac{v^2}{\sqrt{(2kT/m)^2}} \cdot e^{-\frac{mv^2}{k \cdot T}} dv$$

T is the absolute temperature and k Boltzmann's constant. The above equation is applicable for all directions in space. However, we are only interested in the distribution of speed in the direction of the capillary. Using $v^2 = v_x^2 + v_y^2 + v_z^2$ we obtain for the direction x :

$$\frac{n(v_x)}{N} = \sqrt{2kT/m} \cdot e^{-\frac{mv_x^2}{k \cdot T}} dv_x$$

An observer with a fixed position will now see the absorption or emission frequency shifted, due to Doppler's effect (Ch. Doppler: Abh. d. K. Boehmischen Ges. d. Wiss. (5). Vol. II (1842) P. 465), and the value of the shift will be:

$$\nu = \frac{\nu_0}{1 \pm v/c} \text{ assuming } v \ll c$$

ν_0 is the absorption or emission frequency of the resting Neon atom and c the speed of light. If the Doppler equation is used to substitute the velocity v in the Maxwell-Boltzmann velocity distribution the line broadening produced by the movement of Neon atoms can be found. Since the intensity is proportional to the number of absorbing or emitting Neon atoms, the intensity distribution will be:

$$I(\nu) = I(\nu_0) \cdot e^{-\left(\frac{\nu - \nu_0}{\nu_0 \cdot v_w}\right)^2}$$

v_w is the most likely speed according to:

$$v_w = \sqrt{\frac{2kT}{m}}$$

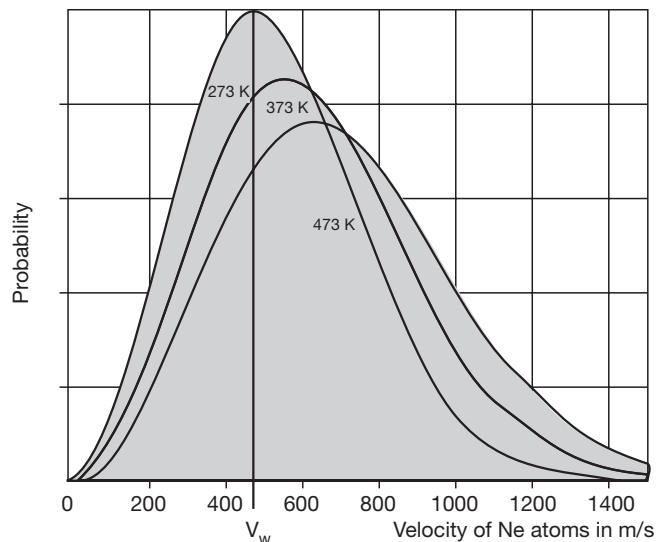


Fig. 10: Probability distribution for the velocity v of the Neon atoms at an interval v to $v+dv$.

The full width at half maximum is calculated by setting $I(\nu_0) = 1/2 I(\nu_0)$ and the result is:

$$\Delta \nu_{\text{doppler}} = \sqrt{4 \cdot \ln 2} \cdot \frac{v_w}{c} \cdot \nu_0$$

From the above equation we can conclude that the line broadening caused by Doppler's effect is larger in the case of:

- higher resonance frequencies ν_0 or smaller wavelengths ($\nu_0 = c/\lambda_0$, UV-lines)
- higher most likely velocity v_w which means higher temperature T

and smaller in the case of:

- a larger particle mass.

The line profile $I(\nu)$ also corresponds to a Gaussian distribution curve. Fig. 11 shows this kind of profile. The histogram only approaches the distribution curve when the speed intervals $d\nu$ are small.

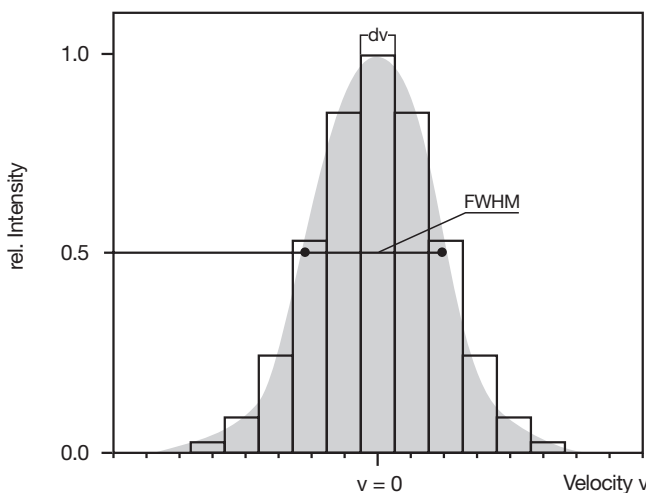


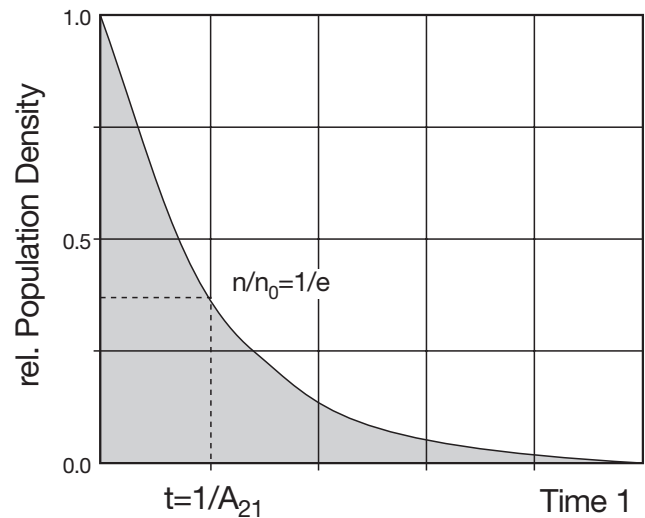
Fig. 11: Inhomogeneous line profile, speed intervals $d\nu$.

On closer observation we can see that a line broadened by the Doppler effect actually does not have a pure Gaussian distribution curve. To understand this, we pick out an ensemble of Neon atoms whose speed components have the value ν in the direction we are looking at. We expect that all these atoms emit light with the same frequency ν or wavelength λ . But we have to consider an additional effect which is responsible for the natural linewidth of a transition. We know that each energy level poses a so-called life time. The population n_2 of a state 2 decays into a state 1 with lower energy with a time constant τ_s following the equation:

$$n_2(t) = n_2(t=0) \cdot e^{-A_{21} \cdot t} \quad \text{with } \tau = 1/A_{21}$$

A_{21} is the famous Einstein coefficient for the spontaneous emission.

Fig. 12 Decay of the population of state 2 into state 1 with lower energy.



This shows us, that the ensemble of Ne atoms does not emit light at a single frequency. It emits a frequency spectra represented by a Lorentz profile (Fig. 13).

$$\delta(\nu) = \frac{1}{4\pi \cdot (\nu - \nu_{21})^2 + (1/2 \cdot \tau_s)^2}, \quad \nu_0 \equiv \nu_{21}$$

The exact profile formation can be determined from the convolution of the Gaussian profile with the individual Lorentz profiles. The result obtained in this manner is known as the Voigt profile. Since one group of particles in an ensemble can be assigned to a given speed ν , these groups have characteristics that differentiate them. Every group has its own frequency of resonance. Which group a photon interacts with depends on the energy (frequency) of the photon. This does not affect the other groups which are not resonant on this interaction. Therefore such kind of a gain profile is termed inhomogeneous.

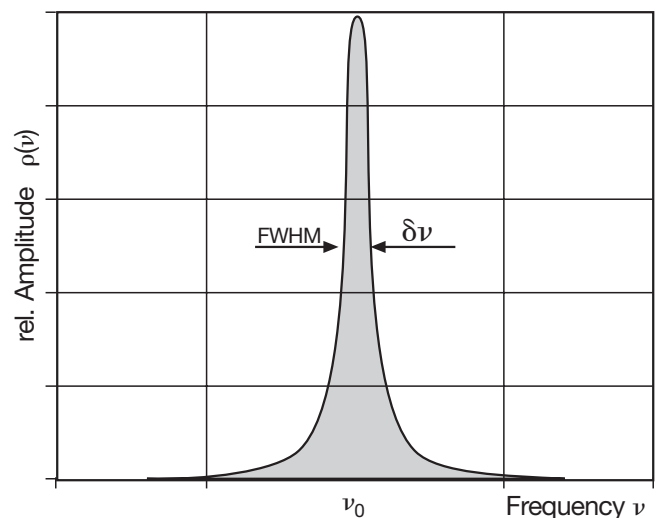
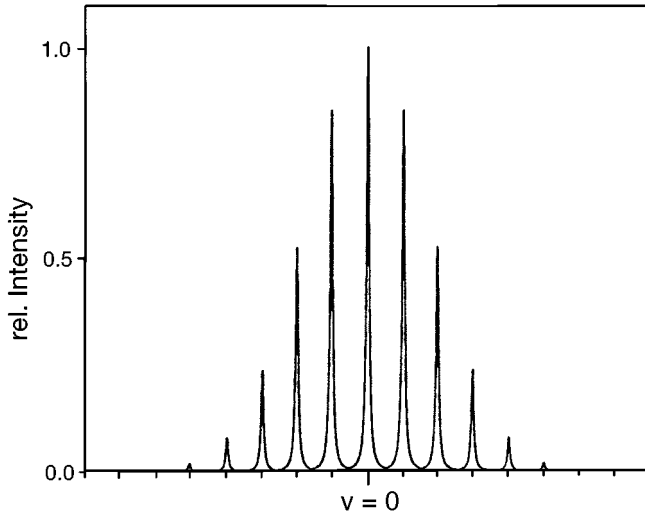


Fig. 13: Natural linewidth (FWHM) caused by spontaneous emission.

Fig. 14 Natural broadened line profiles (homogeneous) for groups of speed v within the inhomogeneous Doppler broadened gain profile.



As we already know a gain occurs in a medium when it shows inversion. This means that the population density of the upper level n_2 (3s in the Ne-system) is larger than the population density of the lower state n_1 (2p). In Fig. 15 the population profiles are rotated by 90° to draw them in the well known energy level diagram. Transitions can only take place between sub-assemblies which have the same velocity v because the optical transition does not change the speed of the particular Ne atom. The situation of Fig. 15 shows a population inversion $n_2 > n_1$. Besides some specific other constants the gain is proportional to the difference $n_2 > n_1$. Now we will place the inverted ensemble of Ne atoms into an optical cavity, which is formed by two mirrors having the distance L . Due to the spontaneous emission photons are generated which will be amplified by the inverted medium and reflected back from the mirrors undergoing a large number of passes through the amplifying medium. If the gain compensates for the losses, a standing laser wave will be built up inside the optical resonator.

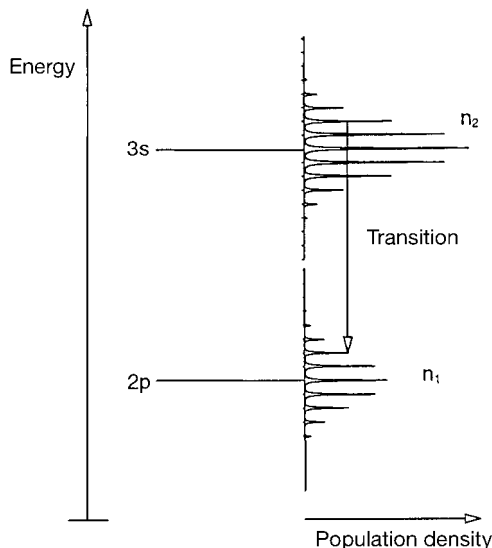


Fig. 15: Population inversion and transition between sub-ensembles with same velocity v .

Such a standing wave is also termed as oscillating mode of the resonator also eigenmode or simply mode (longitudinal mode). Every mode must fulfil the following condition:

$$L = n \cdot \frac{\lambda}{2} \text{ or } L = n \cdot \frac{c}{2\nu}$$

L represents the length of the resonator, λ the wavelength, c the speed of light, ν the frequency of the generated light and n is an integer number. Thus every mode has its frequency of

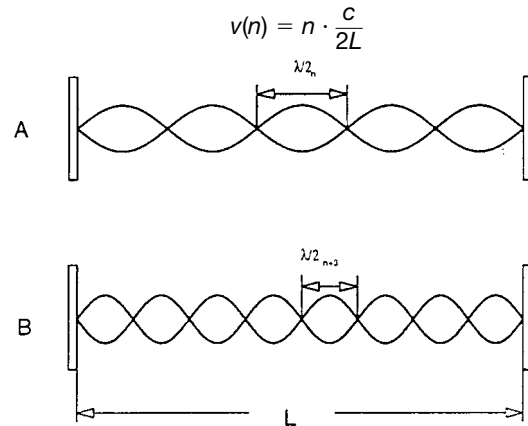


Fig. 16: Standing longitudinal waves in an optical resonator. A with n nodes and B with $n+3$ nodes.

e.g. a He-Ne laser with a resonator length of 30 cm at an emission wavelength λ of 632.8 nm will have the following value for n :

$$n = \frac{\nu}{c} \cdot 2 \cdot L = 2 \cdot \frac{L}{\lambda} = 2 \cdot \frac{0.3}{632.8 \cdot 10^{-9}} = 949.167$$

The difference in frequency of two neighbouring modes is:

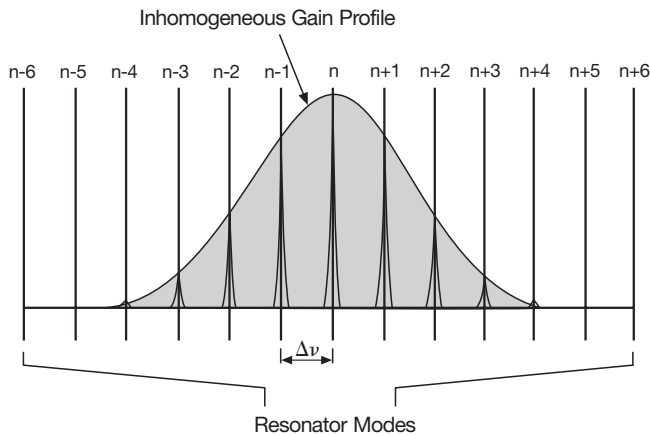
$$\Delta\nu = \nu(n+1) - \nu(n) = (n+1) \cdot \frac{c}{2L} - n \cdot \frac{c}{2L} = \frac{c}{2L}$$

In the above example the distance between modes would be

$$\Delta\nu = \frac{3 \cdot 10^8}{2 \cdot 0.3} = 5 \cdot 10^8 \text{ Hz} = 500 \text{ MHz}$$

If the active laser material is now brought into the resonator standing waves will be formed due to the continuous emission of the active material in the resonator and energy will be extracted from the material. However, the resonator can only extract energy for which it is resonant. Strictly speaking, a resonator has an indefinite amount of modes, whereas the active material only emits in an area of frequency determined by the emission line width. Fig. 17 shows the situation in the case of material that is inhomogeneously broadened.

Fig. 17: Inhomogeneous gain profile (Gaussian profile) interacting with an optical resonator.



If the laser is operating in a stationary state, we can see that it is emitting several longitudinal modes. These are exactly the same modes that will be found in the emission profile. Since the modes are fed by an inhomogeneous emission profile they can also exist independently. The He-Ne laser is a classic example of this.

Lasers that are continuously variable from UV to IR, are probably the dream of every laser physicist. There has been a lot of research in this area and some goals have been partially achieved. Birefringent crystals are used as optical retarder and as tuning elements. A simple model will be used to explain how a birefringent crystal works as a wavelength selecting element.

Light will be observed as an electromagnetic oscillation. We consider the optical component (birefringent crystal) as a collection of many dipoles. These dipoles are determined by the type and form of the electron shells which each atom or molecule has. These dipoles are excited by the electromagnetic field of the light and are thus turned out of their equilibrium (susceptibility). The dipoles absorb energy of the light (virtual absorption) and send it out again. However, a dipole cannot send its beam in the direction of its own axis. If a crystal has two kinds of dipoles, which are at a particular angle to each other, they can only emit and absorb light within the area of their angles. If the process of absorption and emission is slower in one kind of dipole than in the other there will be a phase shift. Macroscopically it seems as if there were a higher refractive index. A change in beam direction takes place because of the different dipole directions, i.e. there are two separate beam directions within the component. If a parallel light beam penetrates into this kind of material the result is, indeed, two beams leaving the crystal. In this case both beams are polarised perpendicularly to each other and have a phase shift between each other.

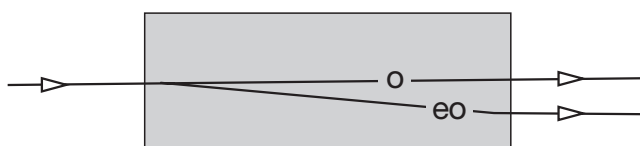


Fig. 18: Birefringent crystal.

This phenomenon is called birefringence. These two marked directions of the crystal also have two distinctive refractive indices. Since one beam appears to be violating Snell's law, it is called extraordinary (eo) and the one behaving normally is called ordinary (o). Crystal quartz and calcite are materials which behave in this way. There is also a series of other crystals but these two have proved successful in laser technology. Thin plates used as optical retarders are mostly made out of quartz because it is hard enough for this purpose. Mica sheets have also been used but they are not suitable for use inside the resonator because of the losses involved. Please note that only crystal quartz has a birefringent behaviour. Quartz that has already been melted (Quartz glass) loses this quality. A whole series of laser components are made out of calcite. Short calcite crystals are sufficient to produce the required beam separation because of the great difference between the ordinary and the extraordinary refractive indices.

A birefringent plate made out of crystal quartz can be used in the He-Ne experimental laser for selecting the wavelengths. This kind of element is also known as a birefringent filter or birefringent tuner. The arrangement within the laser is shown in Fig. 19.

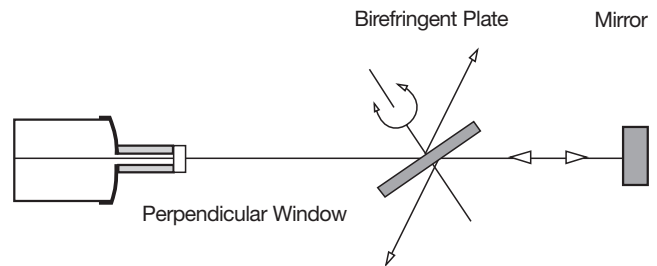


Fig. 19: Birefringent filter for wavelength selection inside the resonator.

The birefringent plate is placed under the Brewster angle into the resonator of the He-Ne laser to avoid reflection losses through the plate itself. The laser can only oscillate in the direction of polarisation given by the birefringent plate itself. The birefringent plate does not change the polarisation if a phase shift of $\delta = 2 \pi$ occurs between the ordinary and the extraordinary beam after passing through it twice. In this case there will be no reflection losses at any plate orientated under the Brewster angle. The phase shift caused by the plate is calculated as follows. The optical path of the ordinary beam is

$$l_o = d \cdot n_o$$

The path of the extraordinary beam is

$$l_{eo} = d \cdot n_{eo}, \text{ so} \\ l_o - l_{eo} = d \cdot (n_o - n_{eo})$$

The phase shift δ is:

$$\delta(\theta) = \frac{2\pi}{\lambda} \cdot 2 \cdot d \cdot (n_o - n_{eo}(\theta))$$

after passing through twice, where d is the geometric path followed by the beam in the plate with thickness d and θ is the angle between the electric field vector of light and the optical axis of the crystal lying in the plane of the plate. When

$$\delta(\theta) = \frac{2\pi}{\lambda} \cdot 2 \cdot d \cdot (n_o - n_{e0}(\theta)) = 2\pi$$

there are no losses. This applies to a given wavelength for a particular angle θ since the thickness of the plate has been preselected.

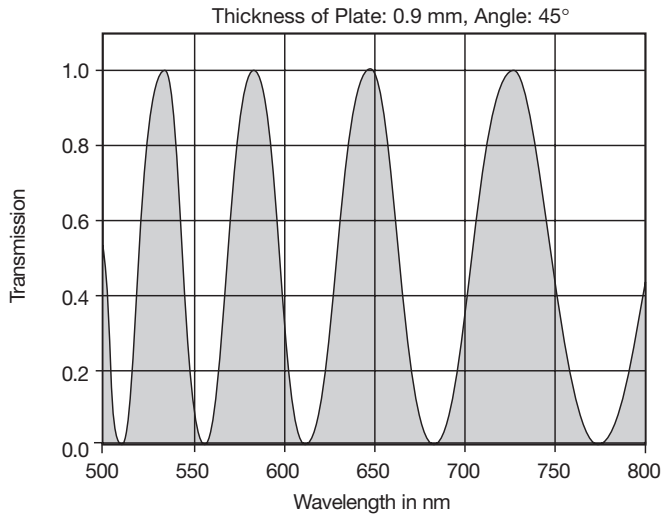
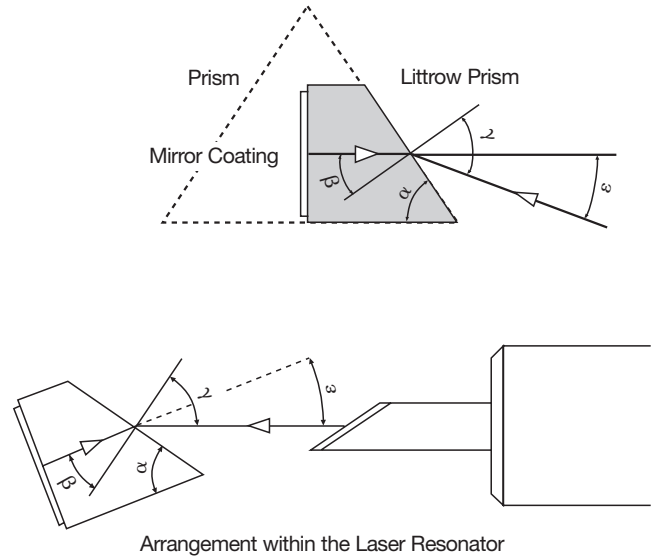


Fig. 20: Transmission of a BFT with a plate thickness of 0.9 mm, an angle of 45° between the electrical field vector and the optical axis calculated for a wavelength range of 500–800 nm. The dispersion of the birefringent quartz was taken into account in this case. This is why the transmission curve changes to higher wavelengths.

Another tuning element is the Littrow prism. Littrow's idea is simple, therefore it is also ingenious. He produced a prism in which the refractive angle is measured in such a way that, in the arrangement of the minimal deviation (beam runs parallel to the hypotenuse), the beam enters the prism just under the Brewster angle. In this way, there are no reflection losses. This kind of prism is also known as a Brewster prism. Littrow then took the prism apart by cutting it down the middle and coated the ensuing surface with a highly reflecting substance. If the refractive index of the first layer is similar to the prism material, the Fresnel losses will be considerably reduced and the result will be an element suffering few losses, that can be used inside the resonator to select wavelengths.

Fig. 21: Formation of a Littrow prism out of a Brewster prism and its arrangement inside the resonator for a tube with Brewster windows.



In some areas such as high resolution spectroscopy or interferometric measuring techniques several longitudinal modes in the laser light prove to be very disturbing (coherent length). Selective frequency losses can be brought into the resonator by an etalon and undesirable modes are damped and suppressed in this way.

An etalon is a plane parallel, low quality resonator. The etalon usually consists of an individual glass body whose plane surfaces are well ground and polished, parallel to each other. Just like a normal resonator, an etalon also has modes. However, its modes are considerably broader since the reflection on the plane surfaces is kept low.

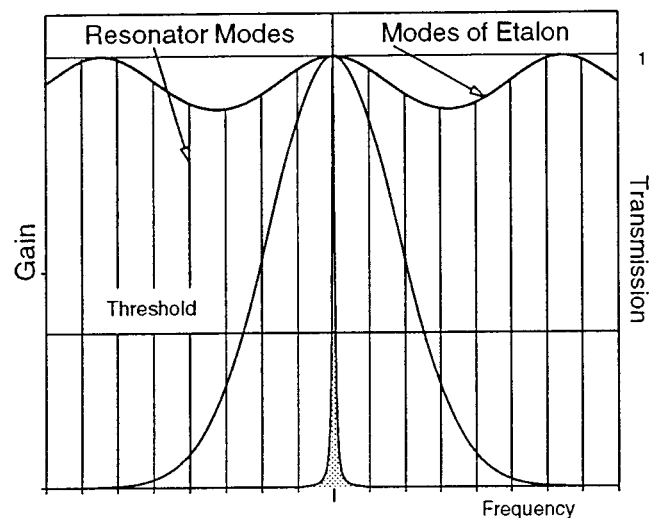


Fig. 22: Mode selection with an etalon.

If the etalon is tilted by the angle γ against the incoming beam the maximum transmission will change according to:

$$Z_m(T = 1) = \frac{2 \cdot d}{m} \cdot \sqrt{n^2 - \sin^2(\gamma)}$$

In this case m is the m -th order, d the thickness of the etalon, n is the refractive index and γ the tilt angle.

According to the above equation the etalon modes can be shifted by tilting the etalon while of course the amplification profile and the resonator modes stay the same. In this way it is possible to encounter more losses in modes that oscillate due to the threshold value amplification than in modes lying just below the maximum transmission.

As in the case of a simple resonator, the distance between the modes is given by the thickness d and the refractive index n :

$$\Delta\nu = \frac{c}{2nd}$$

The etalon must be designed according to the degree of suppression imposed on neighbouring modes and the spectral distance between them. In the He-Ne experimental laser used in the following experiments the etalon is 1 cm thick and does not have any additional coating but only 4 % reflection on each side due to Fresnel losses.

1. The set-up of the He-Ne laser and the adjustment of the resonator mirrors and the tube are technical procedures which have to be elaborated using the instructions outlined in detail within the manual.

The objective of the following experiments is the measurement of:

- The optical stability range of a hemispherical resonator
- The optical output power as a function of the position of the laser tube inside the resonator
- The measurement of the beam diameter inside the resonator

2. The measurement will be carried out while the position of the spherical mirror ($R = 700$ mm) during laser operation is changed up to the stability limit. It can be shifted by slightly loosening the fixing screw on the mirror adjustment support. Be careful that the laser oscillation does not break off due to the shift. The adjustment support is fixed into the new position again and the laser output brought to a maximum by readjustment.

The result of this procedure is shown in Fig. 23. With the laser tube's left end at a distance of 3.5 cm in front of the plane laser mirror the relative output power was measured as a function of the mirror spacing. The right curved mirror is displaced in steps in a way that the mirror spacing varies from 45 to 70 cm. For a spacing of 45 to 55 cm the relative output power increases since the lasing medium available is penetrated by the resonator wave in a more and more optimal way. For a spacing from 55 to 67 cm the diffraction losses in the cavity play a determinant role. Beyond 68 cm the diffraction losses become dominant so that the laser stops oscillating when the spacing reaches the limit of 70 cm.

This spacing is found to be identical with the radius of curvature of the right laser mirror. – The following stability criteria justifies the result of the experiment:

$$-1 \leq g_1 \cdot g_2 \leq 1$$

$$g_1 = 1 - \frac{L}{R_1} \text{ and } g_2 = 1 - \frac{L}{R_2}$$

It is found:

If $R_1 = \infty$ (plane mirror) then the laser power tends to zero by shifting the right mirror to a spacing of $L = R_2 = 70$ cm.

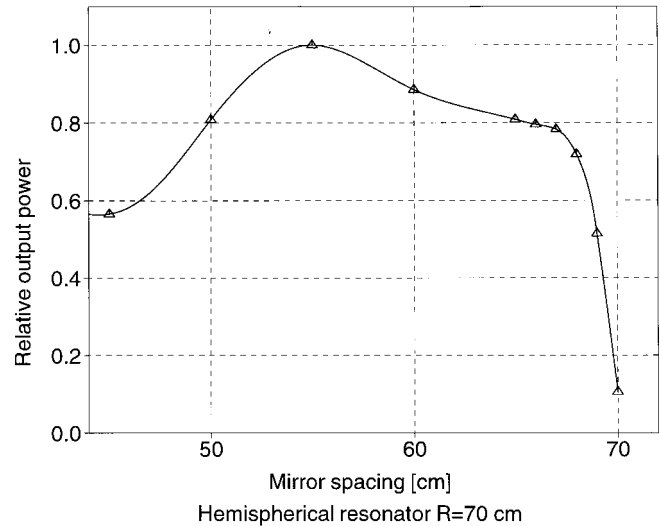


Fig. 23: Relative output power as a function of mirror spacing.

3. The measurement of the output power as a function of the position of the laser tube (capillary) in the resonator is carried out by loosening the fixing screws on the larger carrier which holds the tube and by displacing the tube within the resonator. The resonator is hemispherical with a right mirror of curvature radius $R = 100$ cm. The spacing of the mirrors is 80 cm. The tube is displaced from 20 cm to 60 cm. After each displacement the power is readjusted to maximum by acting on the right mirror and by readjustment of the tube. Fig. 24 shows that the output power has a maximum if the tube is near the plane mirror, i.e. in that part of the resonator where the resonator has its smallest diameter. Here the "mode volume" of the tube is used in an optimal way.

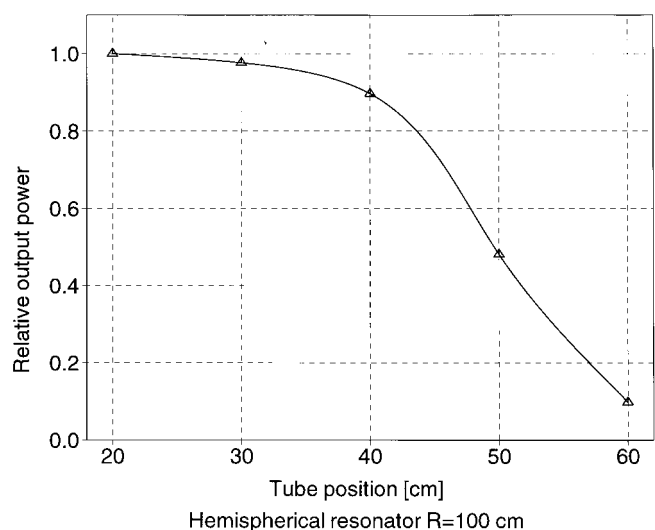


Fig. 24: Relative output power versus tube position in the resonator.

4. The beam diameter is measured within the resonator with the tube at a distance of 30 cm from the plane mirror. The spacing of the mirrors is 90 cm and the radius of curvature of the right mirror is 100 cm. To measure the beam diameter at a particular position a caliper gauge is used as a measuring slit. The caliper gauge is adjusted to approx. 1.5 mm and placed in the beam path. It is moved back and forth and we then observe whether the laser oscillation returns or not. If it does, the value on the adjusted "slit" is reduced till the laser does not oscillate any more. The last value at which laser operation was observed is read from the caliper gauge and noted. This value is the beam diameter at that point. These measurements are repeated at different points and a diagram beam radius versus distance from plane mirror as shown in Fig. 25 should be drawn and compared with the radius $w(z)$ of a Gaussian beam.

5. From Fig. 25 we find for the radius w_0 at the waist a value of 0.28 mm. As shown in the manual the divergence $\tan\theta$ can then be calculated using the relation

$$\tan\theta = \lambda / \pi w_0$$

Hence $\tan\theta = 633 \cdot 10^{-9} / \pi \cdot 0.28 \cdot 10^{-3}$
and $\tan\theta = 0.72 \text{ mrad}$

Therefore the total divergence is 1.44 mrad.

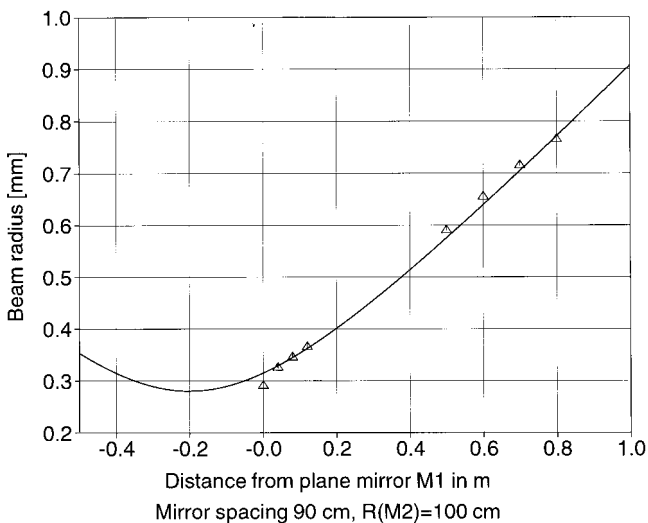
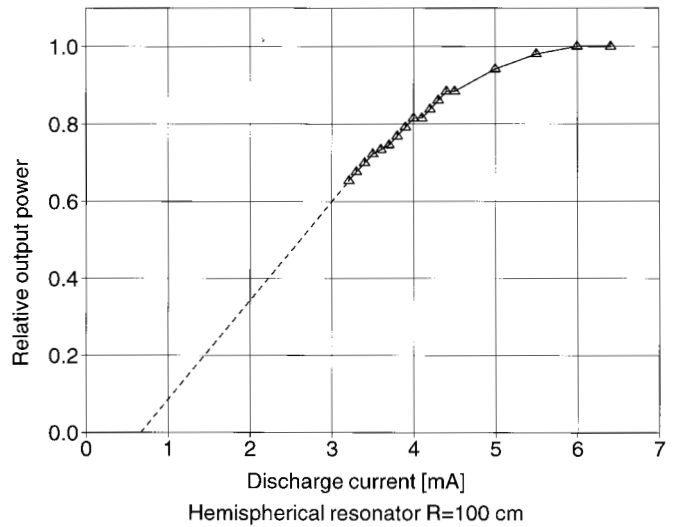


Fig 25: Beam radius within the resonator.

6. In Fig. 26 the relative output power is shown as a function of the tube current. The continuous increase of the tube's current does not increase the output power correspondingly. For currents higher than 6 mA the increase of the electron flux (current) is harming the inversion rather than favouring it. Moreover it can be seen that there is a threshold current needed to get laser power out at all.

Fig 26: Relative laser output power as a function of the discharge current.



Further experiments like wavelength measurements or selection of longitudinal modes can be executed if a monochromator or an analysing Fabry Perot interferometer are available. If a monochromator is available wavelength selection by a BFT and /or LTP-element (tuning) can be performed quantitatively. The laser either has undesirable wavelengths due to its specific characteristics or it suppresses wavelengths which only oscillate when a certain wavelength does not oscillate. The latter is true of the visible lines and a part of the infrared lines of the He-Ne laser. Since the visible lines all start from the same level these lines compete with each other. The line with the lowest threshold energy oscillates first and uses the inversion for its own purposes. The wavelengths of different gain which can be selected by means of the kit's elements are listed below.

- a) 640.1 nm
- b) 635.2 nm
- c) 632.8 nm
- d) 629.8 nm
- e) 611.8 nm

The 611.8 nm line is orange. As a line with small gain it will only oscillate if the supply current is smaller than 5 mA. For currents superior to 5 mA the electron flux disturbs the inversion in a non-acceptable way.

When using a Littrow prism for tuning (LTP) the separation of lines occurs in two ways. One is through dispersion and the other through geometric length, which is still feasible when carried out between the prism and the laser mirror belonging to it. If the lines are wide apart (approx. 20–30 nm), then distances of 5–10 mm (Littrow prism) are great enough for the separation to occur. Lines lying closer together can only be separated by a series connection of several prisms. The basic adjustment of the Littrow prism is described in the manual.

The Littrow prism is used instead of the plane laser mirror and it fulfils two requirements. It works as a prism for wavelength separation and as a plane laser mirror. Strictly speaking it should be possible to select all the lines of the He-Ne laser for which the coating of the surface of the Littrow prism is suit-

able. The lines are tuned by tilting the prism. In case the coated surface of the prism directly vertical to the optical axis of the resonator corresponds to the expected laser oscillation the line selected should also oscillate. In fact, this is not the case. We can observe that the dominant "red line" is still oscillating in spite of tilting the prism. However, the beam path in the resonator changes (we can observe this at the spherical mirror). The laser beam wanders in the resonator as well, so in spite of increasing losses, the amplification of the dominant line is sufficient and the others will not be made to oscillate. "Beam walking", an adjustment procedure in which the beam position in the resonator is changed, can be used to push the dominant line to such an extent on the edge of the possible oscillations that the orange line starts oscillating by further tilting the Littrow prism. "Beam walking" is carried out by slightly turning an adjustment screw on the laser mirror adjustment support and readjusting the output to a maximum by turning the opposite adjustment support in the same direction (x or y). Now the beam changes its direction in the resonator. The iris effect of the capillary stops it from going too far. The objective of the experiment is to understand wave selection with a prism, on the one hand and to get to know the concept of "beam walking" on the other.

For selection of longitudinal modes the etalon is used as a highly precise quartz glass body produced in a parallel fashion. The thickness is 10 mm and the surfaces are not coated. The etalon is mounted in an adjustment support and can be tilted perpendicularly to the axis of the resonator. The etalon is placed into the well adjusted hemispherical resonator. Estimating at sight, the etalon is adjusted horizontally and vertically. After placing the etalon into the resonator the laser should oscillate again. The etalon is now adjusted to the extent that it is perpendicular to the laser beam. We can observe this in return reflections of the etalon and in the increased laser output. Now the etalon is used at the zero order. By tilting it either horizontally or vertically the laser oscillation is stopped at first and starts oscillating at a particular tilt of the etalon. The first order $m = 1$ has been reached. By tilting the etalon even further higher orders are reached. The output power for every arrangement is measured and the result is discussed. If a Fabry Perot is available for analysis the single mode operation can be examined. The continuous tuning of the He-Ne laser within its amplification profile will be observed. The variation in amplitude of the mode while tuning (slight tilting of the etalon) gives you the envelope of the gain profile of Ne.